ENGINEERING

Optical manipulation of work function contrasts on metal thin films

Sai Kishore Ravi,[1] Wanxin Sun,[2] Dilip Krishna Nandakumar,[1] Yaoxin Zhang,[1] Swee Ching Tan[1]*

Work function is a crucial metric in every optoelectronic device to ensure a specific charge transport scheme. However, the number of stable conductive materials available in a given work function range is scant, necessitating work function modulation. As opposed to all the previous chemical methods of work function modulation, we introduce here an alternative approach involving optical modulation. The work function is the minimum energy needed to eject an electron from a solid into vacuum and is known to be light-intensity–independent. A "light intensity dependent" change in work function was observed in metallic thin films coated on a semiconductor. This new phenomenon, contrasting the existing notions on work function, was tested and affirmed with three different systems, namely, Au/n-Si, Pt/n-Si, and W/n-Si. A work function shift of 0.22 eV is achieved in the Pt/n-Si system merely by tuning the illumination intensity from 0 to 18 mW/cm^2. Continuous tuning of work functions to a specified range is now possible just by tuning the light intensity with a few discrete metals in hand. Moreover, selective illumination creates a work function contrast on the metal film, enabling in-plane charge transport. This throws new light on the design and understanding of the optoelectronic devices. In light of this, we also present a simple photodetector design that is sensitive to illumination direction.

INTRODUCTION

Emerging thin-film optoelectronic devices including organic photovoltaics, photodetectors, polymer light-emitting diodes, and optoelectronic prosthetic skins hold a great economic potential for future consumer electronics (*1*, *2*). The quest for superior performance in these devices necessitates effective ways to tailor the electronic structure and optical properties. The advent of band structure engineering is a great leap in the history of the semiconductors and optoelectronics industry. Developing modern optoelectronic materials crucially depends on the choice of electron- and hole-transporting materials and on the tunability of the electronic energy levels and, more importantly, their work function (WF) (*3*–*6*). Fine-tuning WF is paramount in deciding the charge transport scheme and charge kinetics governing the device performance and efficiency (*3*, *4*, *7*). The WFs of the electrode materials is pivotal in photocatalytic and photoelectrochemical systems because it crucially affects the redox properties and hence charge transfer to and from an electrolyte (*8*–*10*). WF tunability has also spurred immense interest in the area of topological insulators (*11*).

Being deterministic of the ultimate device performance, the properties of the interfaces formed by the active materials also call for appropriate modulation. Electrode WFs is a key metric that determines the charge transfer across interfaces in devices. For instance, in any organic optoelectronic device, to achieve an efficient charge transport between the electrode and the active layer, the metal WF needs to match the highest occupied molecular orbital (HOMO)/lowest unoccupied molecular orbital (LUMO) of the organic molecule, which often demands metal WF modulation (*12*, *13*). Most optoelectronic devices require two electrodes of distinctly different WFs with at least one electrode that has a WF low enough to either inject electrons into or collect electrons from the LUMO of an organic molecule (*2*). In bulk heterojunction (BHJ) solar cells, the BHJ active layer is sandwiched between a hole conductor–coated transparent anode and a metal cathode. To work, the metal cathode should have a WF low enough to collect the electrons from the BHJ, whereas the anode should have a high WF to collect the holes (*14*). In inverted structure solar cells, high-WF metals are used as the anode to collect holes, whereas transparent cathodes are used to collect electrons (*15*). Tuning the WF of the electrodes is paramount in these solar cells because the difference in WF between the anode and cathode affects the open-circuit voltage and, hence, power conversion efficiency. In perovskite solar cells, the interface formed by the hole extraction layer and the perovskite is crucial because any energy loss at the interface would be futile. To overcome such losses and to boost the built-in potential, the hole extraction layers should have a high WF to match the ionization potential of the perovskite (*16*). Depending on the WF of the electrode, the nature of interface it forms with an active material in a device is determined. Although it is highly desirable to have an ohmic contact at the interface of the hole extraction layer and the electrode in an organic solar cell, in certain other devices, a Schottky contact would be desirable. For instance, a small Schottky barrier is expected at the interface of a semiconductor and a metal in a field-effect transistor (FET). As a specific example, in a WSe_2-based FET, a metal electrode should have a sufficiently low WF close to the electron affinity of the WSe_2 so as to result in a short Schottky barrier and, hence, a high-performance FET (*17*).

In the design of an optoelectronic device, a number of conditions are often imposed on the choice of the electrode materials in addition to its WF. However, because the number of stable metals with the required WF is limited, it is important to conceive ways to tune the WF to a desired value with the available metals. Although there has been substantial research on ways to enhance conductivity in different classes of electrode materials, research on new ways of WF modulation is rather scant; the electrode WF, though related to conductivity, is, in principle, a distinct property (*18*).

To date, the available routes of WF modulation in the common classes of electrode materials, such as metals, conducting polymers, transparent conductive oxides, and graphene, are predominantly limited to chemical modifications (*2*). Because WF is a property mainly associated with the surface of an electrode material rather than the bulk, its modulation often involves the adsorption of organic layers onto

[1]Department of Materials Science and Engineering, National University of Singapore, 9 Engineering Drive 1, Singapore 117574, Singapore. [2]Bruker Nano Surface Division, 11 Biopolis Way #10-10, The Helios, Singapore 138667, Singapore.
*Corresponding author. Email: msetansc@nus.edu.sg

the surface that form a highly ordered array of molecular dipoles. The organic film has a nonzero effective dipole moment depending on the dipole moment of the individual molecules constituting the film and on their electrostatic interactions. As a result, a dipole barrier is built up between the electrode and the organic films (*19*). Self-assembled monolayers (SAMs) of polar molecules such as alkanethiols and perfluorinated alkanethiols are commonly used to modulate the WF of metals, with the former typically used to decrease the WF and the latter tending to increase the WF owing to the presence of a strongly electron-withdrawing fluorine atom (*13*, *20*). Correlations between the WF change and the dipole moment of the surface modifiers have been propounded (*13*, *21*, *22*). In a recent article, the mechanisms underlying WF modulation have been discussed, typically limited to the chemical means (*23*). Although the magnitude of WF change achieved by optical means in this work (0.22 eV) is lower than that achieved through several chemical means (table S1), the concept introduced in this work can be further improved for wider tunability, sensitivity, and reversibility in modifying an electrode WF. Moreover, many chemical methods suffer from poor stability of the modified WF. For instance, certain SAMs used to modify Au are prone to rapid degradation under ambient conditions because the gold–thiolate bond is easily oxidized (*24*). The presence of ultraviolet light and oxygen in the atmosphere is found to degrade the SAMs on Au. Although SAMs on Au are widely studied, the instability of SAMs on different metals has been reported, and this is known to affect the surface electronic properties of the underlying metal (*25*, *26*). To this end, the need to continuously tune the metal WF in a broad range is strongly felt because the choice of WF in stable metals is practically sparse.

Herein, we demonstrate the possibility of tuning the WF of a thin film of metals such as gold, tungsten, and platinum on silicon (n-type) purely by optical means without any chemical modification to the surface. This is achieved by exploiting an underlying Schottky junction (Au/n-Si, W/n-Si, and Pt/n-Si) that is decisive of the extent of charge injection into the Au film from the semiconductor, under illumination. Because it is hard, in many cases, to choose a counter electrode material of a very specific WF for use in photovoltaic and photoelectrochemical cells, the device performance could be better controlled by using a thin Schottky metal film on a semiconductor instead of a stand-alone metal electrode. This helps in controlling the WF of the electrode by tuning the light intensity. Adopting this strategy in building optoelectronic devices can potentially enhance the device performance by means of precisely tuning the WF. Furthermore, we show that it is possible to generate a WF contrast on the surface just by selectively illuminating an area intended to have a WF lower than the unperturbed area, thereby driving an in-plane electron flow from the low-WF region to the high-WF dark region. In most optoelectronic device architectures, the WF of the entire electrode surface is tuned to a desired value to achieve a specific charge transfer with a material layer interfacing the electrode. In such cases where the device often comprises multiple layers of optically active and charge-transporting materials, the charge injection/extraction occurs across the thickness of the device. This sets a restriction on the minimum thickness of the device. In-plane charge transport on an unmodified material surface, with energy levels tuned by nonchemical means, shines a new ray of hope on future device architectures, breaking thickness limitations. Moreover, in special cases such as three-dimensional topological insulators, where the charge transport is desired to be only on the surface, creating in-plane WF contrasts is certainly critical. Very recently, an in-plane topological p-n junction has been created on a three-dimensional topological insulator, where one-half of the surface is chemically modified with the surface chemical potential tuned to result in a p-type zone, leaving the other half of the surface as n-type (*11*). With rather inadequate research on creating an in-plane contrast in the chemical potential or the electronic energy level of a material surface, the present work throws light on a new approach for localized modulation of WF and for in-plane charge transport simply by white light illumination. The shift in WF was found to be dependent on the illumination intensity. Here, we examine the WF contrast on a metal thin film deposited with different thicknesses on an n-type Si wafer. WF is deduced from the contact potential difference (CPD) measured using Kelvin probe force microscopy (KPFM).

RESULTS

Surface photocurrents on partial illumination of metal/n-Si

The system under study involved a Au, W, or Pt thin film coated on a Si substrate with one-half of the metal surface blocked from light while the other half is illuminated (Fig. 1A and movie S1). Under no applied bias, when the two terminals for the electrical measurements were positioned in the dark and bright zones, respectively, a photocurrent of ≈150 μA (Fig. 1B) was observed when one-half of the Au surface was selectively illuminated with a white light of intensity 100 mW/cm^2. Keeping the sample surface and the terminals unchanged, when the dark and bright zones were swapped by illuminating the other half previously concealed, a photocurrent of an equal magnitude but of an opposite polarity was observed (Fig. 1B). It is inferred that there is a directional electron flow on the surface that always flows from the bright to the dark zone. This indicates a change in surface potential induced by illumination. Supporting this, a rise in photovoltage was also observed under identical conditions of partial illumination (Fig. 1C). On the other hand, when the entire surface was uniformly illuminated, the photocurrent and photovoltage were significantly low (Fig. 1, B and C). Similar photoresponses were also observed in W-Si and Pt-Si systems (fig. S1). To examine the effect of the film thickness, identical photoresponse measurements were conducted on samples with ≈15-, 60-, and 300-nm films of Au sputtered on Si. There was a 33% reduction in photocurrent upon increasing the film thickness from 15 to 60 nm, and there was more than a fourfold drop in photoresponse when the thickness was further increased to 300 nm. This is suggestive of the role of the underlying Si substrate in driving the photoresponse and the need for the metal film to be thin enough for the photons to reach the Si interface.

Effect of light intensity and metal film thickness on WF contrasts

To corroborate this effect further, CPDs on the films of different thicknesses were measured using KPFM. Illuminating the sample under scan with a white light of ≈18 mW/cm^2 showed a distinct shift in surface potential as opposed to the surface potential under dark scan (Fig. 2, A and B). To check the spontaneity of surface potential shift under illumination, in the course of the KPFM scan, two light ON/OFF cycles were triggered, which resulted in a surface potential map with distinct bright and dark bands corresponding to the cycles of light ON and OFF, respectively (Fig. 2C). In congruence with the photocurrent results, a high surface potential contrast and, hence, a high WF contrast (0.12 to 0.15 eV) were observed in the 15-nm film (Figs. 2D and 3D). Upon increasing the film thickness, the WF shift was greatly reduced (Fig. 3). The WF shift (ΔWF) dropped to 0.08 eV for the 60-nm film, and there was a weak response of 0.03 eV in case of the 300-nm film (Fig. 3, A to D). Because WF contrast is photoinduced, it was intriguing to check

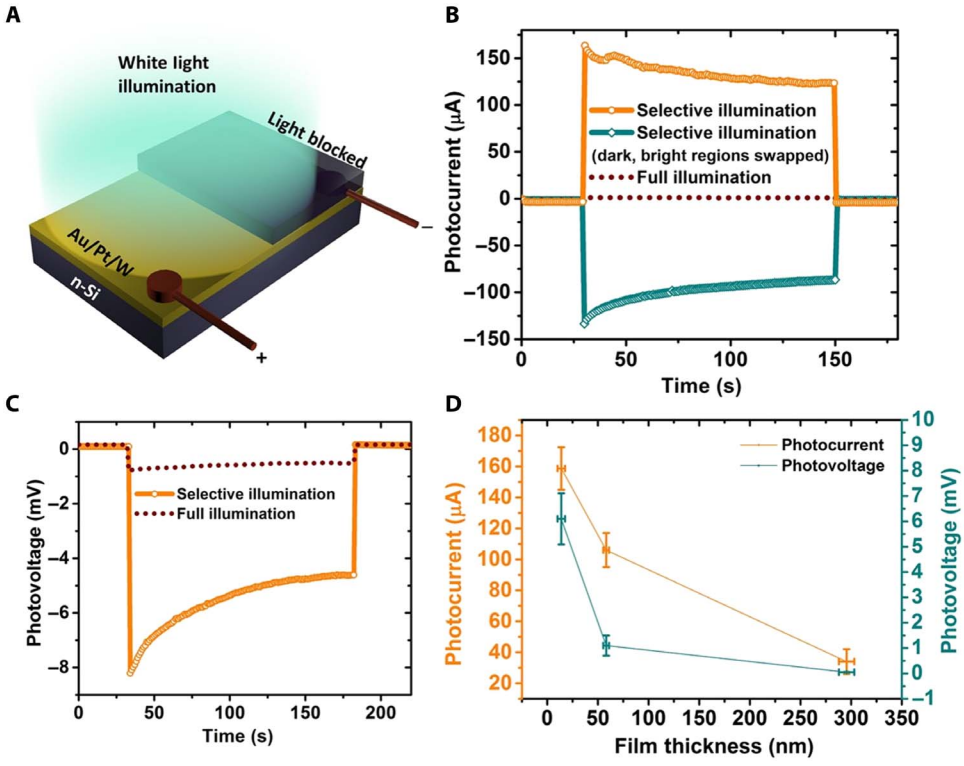

Fig. 1. Photocurrents and photovoltages under partial illumination. (**A**) Schematic showing a semiconductor coated with metal partially illuminated on the surface with the remaining area blocked from light. (**B**) Photocurrent generated in 15-nm Au/n-Si under partial illumination, with the electrons flowing from the bright zone to the dark zone. (**C**) Photovoltage generated under partial illumination in 15-nm Au/n-Si. (**D**) Effect of metal film thickness on the photocurrent.

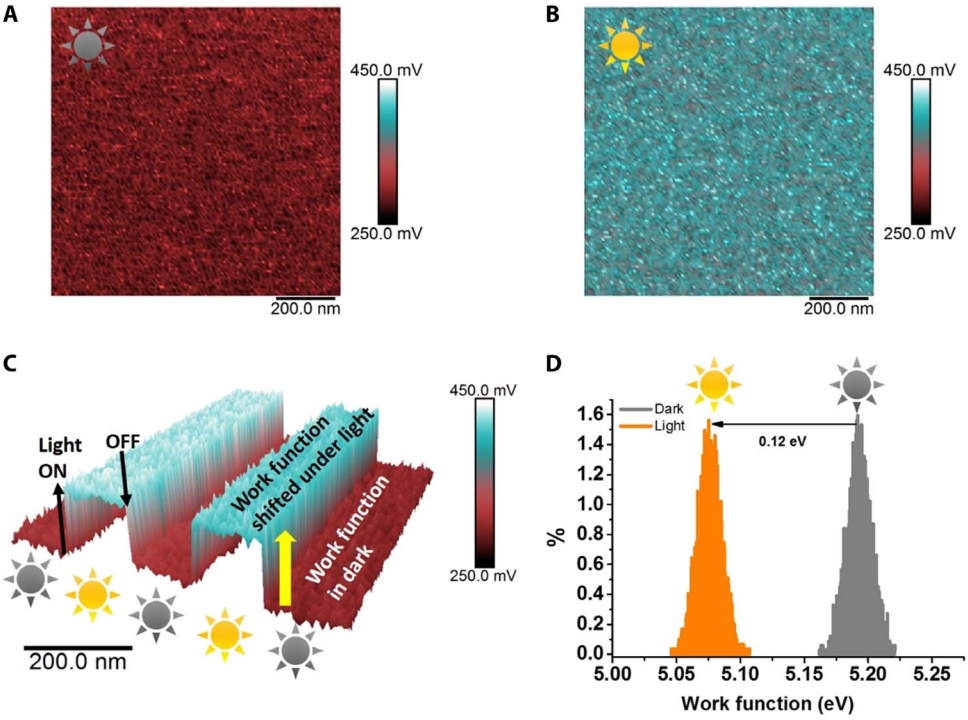

Fig. 2. Effect of illumination on surface potential. (**A** and **B**) Surface potential maps of 15-nm Au/n-Si before (A) and after (B) illumination. (**C**) Surface potential map showing instantaneous photoresponse when two light ON/OFF cycles were triggered, which resulted in a surface potential map with distinct bright and dark bands corresponding to the cycles of light ON and OFF. (**D**) WF shift determined from the surface potential histograms corresponding to the bright and dark scans. The peak of the histogram being the average WF, the peak-to-peak distance gives the average WF shift.

whether the WF can be optically modulated by tuning the light intensity and whether the trend can be applied to multiple metal-semiconductor systems. A clear decreasing trend in ΔWF is seen as the light intensity is decreased from 18 to 0.04 mW/cm^2 (Fig. 4A). A similar trend is observed in other Schottky systems such as W/n-Si and Pt/n-Si (Fig. 4, B to D). To confirm the role of metal-semiconductor systems, a similar KPFM scan was run on a plain n-Si wafer with two cycles of illumination and darkness, where no WF shift was observed (fig. S2)

Origin of WF contrasts

An explanation for this photoinduced WF contrast and the ensuing in-plane charge transport could be obtained by studying the nature of the metal-semiconductor interface. As dictated by the WF of the semiconductor (φ_{Si}) and the metal (φ_m) before contact, either a Schottky junction (for $\varphi_m > \varphi_{Si}$) or ohmic junction (for $\varphi_m < \varphi_{Si}$) is formed on contact. As for most noble metals, the WFs of Au, W, and Pt are greater than that of the n-type Si before contact. As the metal and the semiconductor are brought into contact, the electrons from Si diffuse into the metal, which has a deeper Fermi level, leaving behind holes in Si, resulting in negative charge accumulation near the metal and positive charge accumulation in Si. As a result, the free electrons are preferentially depleted in Si near the metal/Si junction as compared to the bulk, forming a depletion region in Si near the interface, leading to band bending. A Schottky barrier is formed at the interface as the Si energy

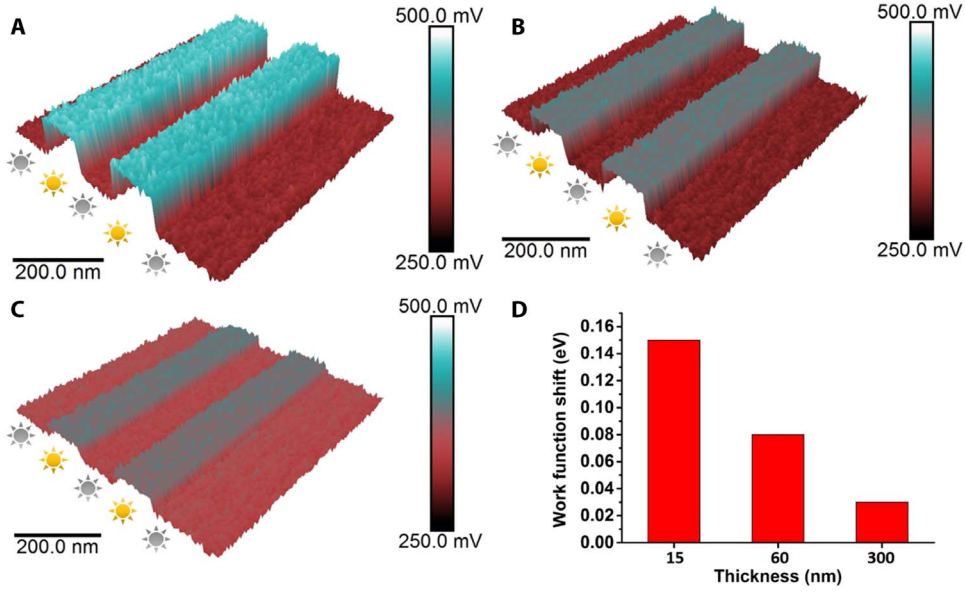

Fig. 3. Effect of film thickness. (**A** to **C**) KPFM (CPD) plots for Au films of thickness 15 nm (A), 60 nm (B), and 300 nm (C) on Si. (**D**) Effect of film thickness on the WF shift.

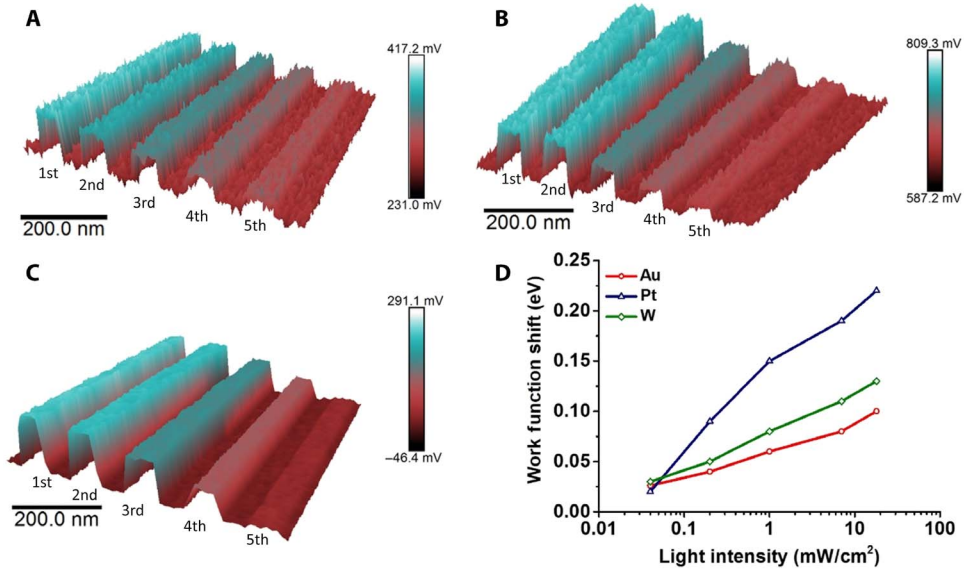

Fig. 4. KPFM on different metallic thin films. (**A** to **C**) CPD plots for Au (A), W (B), and Pt (C) films under different illumination intensities. Each CPD map has five step-like features (first to fifth), with the first step being the highest surface potential shift (left most) under 18 mW/cm^2 illumination intensity and the second to fifth steps being the shifts obtained, respectively, at light intensities of 7, 1, 0.2, and 0.04 mW/cm^2. (**D**) Effect of light intensity on the WF shift.

band bends upward toward the metal, bringing the Fermi levels of the metal and Si to an equilibrium. The depletion region has an internal electric field that tends to drift the electrons toward the bulk of the semiconductor and the holes into the metal. Under illumination, the electrons are excited into the conduction band (CB) of Si [leaving holes in the valence band (VB)], and during the initial stages of photoexcitation, the electron-hole pair enters the depletion region and is subjected to the internal electric field that drifts the CB electrons into the Si bulk while expelling the VB holes into the metal. However, under continuous illumination, electrons continue to accumulate in the Si CB near the barrier. These electrons gain sufficient kinetic energy (henceforth called "hot electrons") to overcome the Schottky potential barrier and are injected into the metal (Fig. 5, A and B).

Under dark conditions, the WF of the gold film (≈15 nm) was measured to be −5.2 eV, whereas under illumination (18 mW/cm^2), the WF shifts to −5.1 eV (Fig. 4, A and B). Similarly, under illumination, the WFs of Pt and W thin films rose to −5.3 and −4.7 eV, respectively, from −5.5 and −4.8 eV. This in essence indicates the shortening of Schottky barrier height (SBH) under illumination. The photocurrent observed on illuminating one-half of the metal/Si sample (leaving the other half blocked to light) is attributed to this WF contrast on the Au surface that drives the in-plane charge transport. The photoexcited electrons accumulating at the Schottky barrier that gain sufficient kinetic energy to become hot electrons surpass the energy barrier and inject into the metal. The photoinduced hot electrons injected into the metal are at a lower WF (φ_m*) in the illuminated region (bright zone) and are transferred to the dark zone, which has a higher WF (φ_m) (Fig. 5C). This in-plane charge transport is deemed to occur from the bright to the dark zone, which is confirmed by the reverse photocurrent observed on swapping the bright and dark zones. The effect of film thickness on the photocurrent is mainly related to the intensity of light reaching the underlying Si surface because Si is the main source of photocarrier generation. As the film thickness increases, the transparency of the film drops, limiting the light reaching the Si and, hence, limiting the number of photocarriers generated (fig. S3). The effect of light intensity on the photocurrent is correlated to the resulting SBH in the Au/Si interface. As

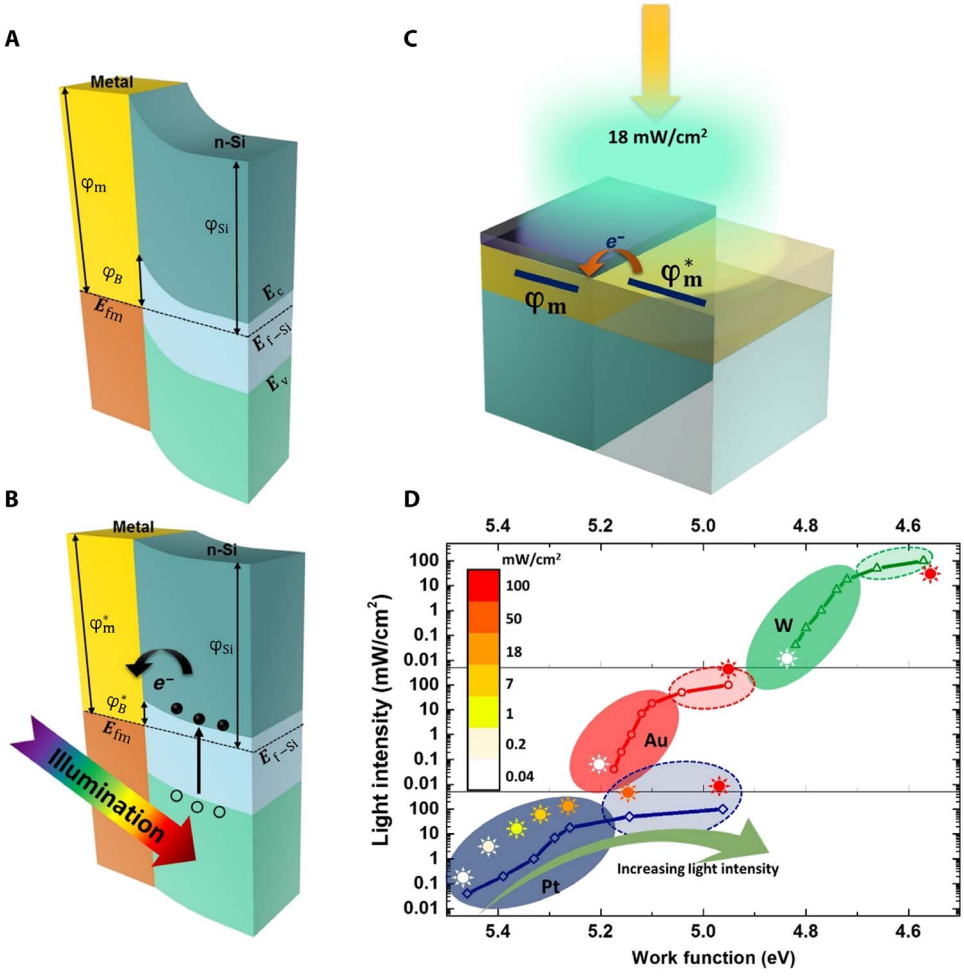

Fig. 5. Band structures of a metal-semiconductor junction forming a Schottky junction. (**A** to **C**) Without illumination (A), with illumination (B), and under selective illumination (C) showing flow of electrons from the bright zone (the region of low WF) to the dark zone (the region of high WF). (**D**) Possibility of continuous tuning of WF by choosing a specific metal and a specific light intensity. The dark ellipses present the experimental WF data under light intensities from 0.04 to 18 mW/cm^2, and the dashed ellipses present a projection of WF under higher light intensities of 50 and 100 mW/cm^2. A projection of data had to be made to estimate the WF shift at 100 mW/cm^2 because the light intensity on the sample surface could not be increased beyond 18 mW/cm^2 in the KPFM setup owing to instrumentation constraints. The projections are made using the linear interpolation/extrapolation program in Origin Pro 8.0 (OriginLab).

the light intensity increases, the SBH decreases, which implies that the excess kinetic potential required by the accumulating electrons to overcome the barrier also decreases. Thus, more hot electrons are injected into the Au owing to the lowered SBH, resulting in a high photocurrent under high light intensity. To support this mechanism, similar photocurrent measurements were conducted on metal films of different thicknesses coated on a thinner silicon wafer with illumination incident on the silicon wafer instead of the metal (fig. S4). Here, because the light reaches the metal film through a fixed thickness of silicon, back illumination from Si is expected to eliminate the thickness effect because it stems only from the reduced light transmission in thick metal films. As expected, the trend of decreasing current flow (indirectly decreasing WF contrast) with increasing thickness disappeared because the light intensity reaching the Au films of different thicknesses became a constant as the light was shined from the Si side. Now, the current flow became higher in thicker films (fig. S4) as they offered lower resistance for current flow for the same magnitude of electron injection (due to the fixed light intensity).

Corroboration of WF contrast

To check for any effect of resistance changes on the metal surface and to verify the WF contrast on the metal surface, current/voltage (*IV*) characteristics of metal films with and without a semiconductor under different conditions were studied. Although, in all photocurrent measurements, the electrical contacts from both terminals were taken only from the gold surface and the silicon substrate was not part of the circuit, the *IV* studies provided further proof of photocurrent on the metal surface and eliminated the possibility of in-plane photocurrent on the silicon surface. The *IV* curves of the metal film on n-Si exhibited an ohmic behavior and did not have any change in resistance under light and dark as opposed to that of plain n-Si (fig. S5, A and B). As expected, the resistance of the plain n-Si wafer was lower under illumination (fig. S5B). Hence, in the setup considered (15-nm Au on Si—with partial illumination), the Si in the dark zone would have a higher resistance and that in the light zone would have a lower resistance. Because the photocurrent direction proves the electron flow from the bright to the dark zone, if the electrons had to flow on the surface of n-Si instead of the metal, then it would imply a flow of electrons from a region of low resistance to that of high resistance, which would not be possible because it is not in agreement with the high photocurrents observed. The resistance of the semiconductor is three orders of magnitude higher than that of the metal film, which indicates that the observed high photocurrents could not be from the Si surface (fig. S5A). Because the metal film on n-Si did not have any change in resistance under light and dark, the in-plane photocurrent is unhindered and driven only by the WF contrast on the partially illuminated surface.

A major applicability of this observation would be in the optoelectronic devices that are exposed to light under operation. Because there has not been any consideration before on the effect of metal WFs under illumination when they are in Schottky contact with a semiconductor, most device designs assume the metal WF to be constant, which makes the knowledge on the device operation less accurate. These observations aid in designing the device considering the effect of illumination intensity especially in photovoltaic devices. Because most photovoltaic devices are tested under 100 mW/cm^2, a projection of the present trend has been estimated for 100 mW/cm^2, as shown in Fig. 5D, which would facilitate better device designs in future. The map (Fig. 5D) shows the possibility of tuning the WF to a specific value over a range of 4.5 to 5.5 eV by simply choosing a combination of a specific Schottky metal and specific light intensity. A projection of data had to be made to estimate the WF shift at 100 mW/cm^2 because the light intensity on the sample surface could not be increased beyond 18 mW/cm^2 in the KPFM setup owing to instrumentation constraints. All KPFM WF measurements were hence performed with an illumination of 18 mW/cm^2, and during the entire period of illumination, the temperature rise was well within 1°C, which eliminates any possibility of thermal effects on WF change (fig. S6).

Application: A proof-of-concept photodetector design

On the other hand, the in-plane charge transport observed as a result of the WF contrast by itself can be applied in a number of photovoltaic and photodetector applications. A simple setup designed as a photodetector (Fig. 6) demonstrates the usefulness of the in-plane WF contrast for practical optoelectronic applications. The metal-semiconductor system (W/n-Si in this case) with two terminals (A and B) from two different ends on the metal surface was positioned in a black chamber with four slots, as shown in Fig. 6A. Although photodetectors typically work based on the sensitivity of the magnitude of the photocurrent to the light intensity, the present design is sensitive to the position of the illumination source in addition to the light intensity. The design is a simple implication of the reversal of the photocurrent polarity on swapping the bright and dark zones, whereby the position of light source is shifted. Note that a high WF contrast between two zones is achieved only when a high light intensity contrast between the two zones is established. When slot 3 is opened for illumination with all other slots closed, a photocurrent of ≈+43 μA was observed, whereas a negative photocurrent of roughly the same magnitude (≈−39 μA) was observed when slot 4 was

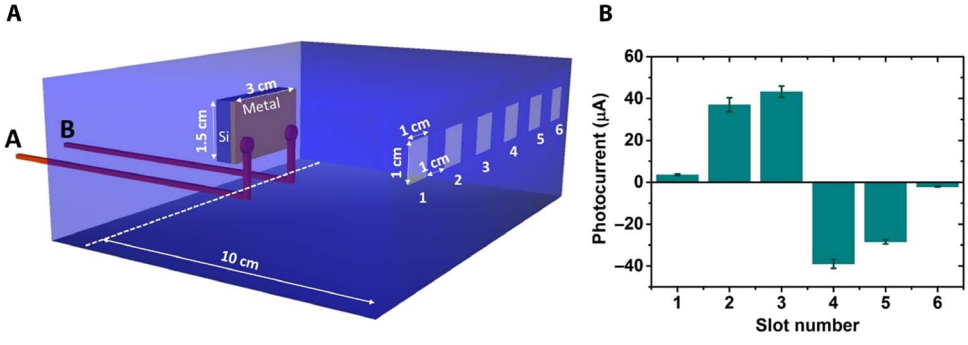

Fig. 6. A proof-of-concept photodetector. (**A**) A photodetector setup showing the dependence of the photocurrent on the position of the light source. The actual chamber used is black and opaque to light, and the schematic shows a transparent chamber for illustrative purposes. (**B**) Photocurrent observed on opening a specific slot (*x* axis) with all the other slots closed.

opened for illumination with all other slots closed. A similar trend was observed with slots 2 and 5, but the magnitude of the photoresponse was lower and the response further decreases in the case of slots 1 and 6. When slot 3 is illuminated, terminal A lies in the bright zone and terminal B lies in the dark zone yielding a positive photocurrent, whereas a negative photocurrent of equal magnitude is observed when slot 4 is illuminated where terminal A is the dark zone and terminal B is the bright zone. This example evinces the sensitivity to the position of the illumination source. When slot 2 is illuminated (with all other slots closed), terminal A is not fully illuminated but is exposed to a relatively higher light intensity as opposed to terminal B, whereas when slot 5 is illuminated, terminal B is exposed to a higher light intensity. A similar positive and negative response is obtained by individually illuminating slots 2 and 5, as obtained for slots 3 and 4, respectively, but the photoresponse is lowered because of the low difference in light intensity between the two terminals. In the case of slots 1 and 6, the photoresponses further dropped (Fig. 6B). The reduction in the magnitude of the photocurrent in the latter two cases is due to the low light intensity contrast resulting in a poor WF contrast. In a nutshell, this photodetector design enables photocurrent to be sensitive to "light intensity contrast" in addition to "absolute light intensity"—owing to the generation of an in-plane WF contrast. A similar effect was observed when the sample was moved in and out of a region of illumination with the illumination source kept unmoved (movie S2).

DISCUSSION

To summarize, the present study demonstrates the possibility of tuning the WF by as high as 0.22 eV by shining light of a moderate intensity (18 mW/cm^2) on a metal-semiconductor Schottky system. A projection of as high as 0.5 eV could be expected under standard illumination conditions (100 mW/cm^2) relevant for photovoltaic applications. The study paves the way for better design considerations in optoelectronic devices, taking the light intensity dependence of WF into account. This also throws light on the possibility of a wider choice of WFs in a given range by simply choosing a combination of a Schottky metal and an illumination intensity, which helps to achieve a very specific WF in the electrode in an optoelectronic device, which otherwise has only a limited choice of WFs with only a few stable metals available in any given WF range.

MATERIALS AND METHODS

The precleaned prime grade n-type silicon wafers (3 cm × 1.5 cm, 525 μm thick) were coated with Au, Pt, or W by using magnetron sputtering for time durations ranging from 60 to 900 s. All comparisons in photocurrents/voltages among the three different metals were made with the lowest film thickness. The average film thickness for all three metals under comparison was maintained at 15 nm. The effect of film thickness has been demonstrated with the Au/n-Si system where the film thickness was increased by increasing the duration of sputtering up to 900 s. Photocurrent/voltage measurements under selective illumination were performed by covering one of the terminals by a thick black paper. The illumination source used for the photocurrent measurements was a standard white light with an intensity of 100 mW/cm^2. All the electrical measurements were performed using Keithley K2400. Photocurrent measurements were also repeated with a back illumination from the silicon side by coating metal films on a thinner Si wafer (3 cm × 1.5 cm, 170 μm thick, n-type).

The KPFM measurements were performed using Dimension Icon (Bruker Nano Surfaces). Amplitude modulation KPFM was used to obtain a high signal-to-noise ratio as opposed to that of frequency modulation. All KPFM measurements were performed in dual pass mode to completely eliminate the topography effect. The Pt/Ir-coated SCM-PIT probes of known WF were used for the KPFM scans. When the tip with an applied bias scans the surface of the sample, a CPD is created between the tip and the sample surface, which was used to quantify the WF as per the equation

$$\mathrm{CPD} = \frac{(\varphi_{\mathrm{tip}} - \varphi_{\mathrm{sample}})}{e^-}$$

where φ_{tip} is the WF of the Pt/Ir tip, which is 5.5 eV, and $\varphi_{\mathrm{sample}}$ is the WF of the sample that is to be determined. Maximum illumination intensity that could be used in the KPFM measurements was limited to 18 mW/cm^2 owing to instrumentation constraints.

SUPPLEMENTARY MATERIALS

Supplementary material for this article is available at http://advances.sciencemag.org/cgi/content/full/4/3/eaao6050/DC1

fig. S1. *IV* characteristics and photobehavior in different metal/n-Si systems.
fig. S2. KPFM surface potential map of a plain n-type Si, which shows no significant WF shift under two cycles of dark and illumination cycles.
fig. S3. Effect of metal film thickness (Au sputtered on glass) on transmittance of light at a wavelength of 600 nm.
fig. S4. Metal thickness effect in case of back illumination.
fig. S5. Light and dark *IV* characteristics.
fig. S6. Temperature profile of Au/n-Si under dark and illumination conditions.
fig. S7. Effect of the relative position of the sample with respect to the illumination zone.
table S1. WF modification in Au, Pt, and W by various chemical methods.
movie S1. Surface photocurrents under partial illumination of metal/n-Si.
movie S2. Sensitivity of photoresponse to the relative position of the sample.
References (*27*–*35*)

REFERENCES AND NOTES

1. T. Yokota, P. Zalar, M. Kaltenbrunner, H. Jinno, N. Matsuhisa, H. Kitanosako, Y. Tachibana, W. Yukita, M. Koizumi, T. Someya, Ultraflexible organic photonic skin. *Sci. Adv.* **2**, e1501856 (2016).
2. Y. Zhou, C. Fuentes-Hernandez, J. Shim, J. Meyer, A. J. Giordano, H. Li, P. Winget, T. Papadopoulos, H. Cheun, J. Kim, M. Fenoll, A. Dindar, W. Haske, E. Najafabadi, T. M. Khan, H. Sojoudi, S. Barlow, S. Graham, J.-L. Brédas, S. R. Marder, A. Kahn, B. Kippelen, A universal method to produce low–work function electrodes for organic electronics. *Science* **336**, 327–332 (2012).
3. M. Schwarze, W. Tress, B. Beyer, F. Gao, R. Scholz, C. Poelking, K. Ortstein, A. A. Günther, D. Kasemann, D. Andrienko, K. Leo, Band structure engineering in organic semiconductors. *Science* **352**, 1446–1449 (2016).
4. D. Veldman, S. C. J. Meskers, R. A. J. Janssen, The energy of charge-transfer states in electron donor–acceptor blends: Insight into the energy losses in organic solar cells. *Adv. Funct. Mater.* **19**, 1939–1948 (2009).
5. K.-Y. Wu, S.-Y. Yu, Y.-T. Tao, Continuous modulation of electrode work function with mixed self-assembled monolayers and its effect in charge injection. *Langmuir* **25**, 6232–6238 (2009).
6. C. G. Tang, M. C. Y. Ang, K.-K. Choo, V. Keerthi, J.-K. Tan, M. N. Syafiqah, T. Kugler, J. H. Burroughes, R.-Q. Png, L.-L. Chua, P. K. H. Ho, Doped polymer semiconductors with ultrahigh and ultralow work functions for ohmic contacts. *Nature* **539**, 536–540 (2016).
7. J. Widmer, M. Tietze, K. Leo, M. Riede, Open-circuit voltage and effective gap of organic solar cells. *Adv. Funct. Mater.* **23**, 5814–5821 (2013).
8. S. Bai, J. Jiang, Q. Zhang, Y. Xiong, Steering charge kinetics in photocatalysis: Intersection of materials syntheses, characterization techniques and theoretical simulations. *Chem. Soc. Rev.* **44**, 2893–2939 (2015).
9. S. K. Ravi, S. C. Tan, Progress and perspectives in exploiting photosynthetic biomolecules for solar energy harnessing. *Energ. Environ. Sci.* **8**, 2551–2573 (2015).

10. V. K. Singh, S. K. Ravi, J. W. Ho, J. K. C. Wong, M. R. Jones, S. C. Tan, Biohybrid photoprotein-semiconductor cells with deep-lying redox shuttles achieve a 0.7 V photovoltage. *Adv. Funct. Mater.* 1703689 (2017).
11. N. H. Tu, Y. Tanabe, Y. Satake, K. K. Huynh, K. Tanigaki, In-plane topological p-n junction in the three-dimensional topological insulator $Bi_{2-x}Sb_xTe_{3-y}Se_y$. *Nat. Commun.* **7**, 13763 (2016).
12. H. Ma, H.-L. Yip, F. Huang, A. K.-Y. Jen, Interface engineering for organic electronics. *Adv. Funct. Mater.* **20**, 1371–1388 (2010).
13. B. de Boer, A. Hadipour, M. M. Mandoc, T. van Woudenbergh, P. W. M. Blom, Tuning of metal work functions with self-assembled monolayers. *Adv. Mater.* **17**, 621–625 (2005).
14. H. Choi, H.-B. Kim, S.-J. Ko, J. Y. Kim, A. J. Heeger, An organic surface modifier to produce a high work function transparent electrode for high performance polymer solar cells. *Adv. Mater.* **27**, 892–896 (2015).
15. A. K. K. Kyaw, D. H. Wang, V. Gupta, J. Zhang, S. Chand, G. C. Bazan, A. J. Heeger, Efficient solution-processed small-molecule solar cells with inverted structure. *Adv. Mater.* **25**, 2397–2402 (2013).
16. K.-G. Lim, H.-B. Kim, J. Jeong, H. Kim, J. Y. Kim, T.-W. Lee, Boosting the power conversion efficiency of perovskite solar cells using self-organized polymeric hole extraction layers with high work function. *Adv. Mater.* **26**, 6461–6466 (2014).
17. W. Liu, J. Kang, D. Sarkar, Y. Khatami, D. Jena, K. Banerjee, Role of metal contacts in designing high-performance monolayer n-type WSe_2 field effect transistors. *Nano Lett.* **13**, 1983–1990 (2013).
18. J. Janata, M. Josowicz, Conducting polymers in electronic chemical sensors. *Nat. Mater.* **2**, 19–24 (2003).
19. M. L. Sushko, A. L. Shluger, Rough and fine tuning of metal work function via chemisorbed self-assembled monolayers. *Adv. Mater.* **21**, 1111–1114 (2009).
20. C.-Y. Chen, K.-Y. Wu, Y.-C. Chao, H.-W. Zan, H.-F. Meng, Y.-T. Tao, Concomitant tuning of metal work function and wetting property with mixed self-assembled monolayers. *Org. Electron.* **12**, 148–153 (2011).
21. D. M. Alloway, A. L. Graham, X. Yang, A. Mudalige, R. Colorado Jr., V. H. Wysocki, J. E. Pemberton, T. R. Lee, R. J. Wysocki, N. R. Armstrong, Tuning the effective work function of gold and silver using ω-functionalized alkanethiols: Varying surface composition through dilution and choice of terminal groups. *J. Phys. Chem. C* **113**, 20328–20334 (2009).
22. N. V. Venkataraman, S. Zürcher, A. Rossi, S. Lee, N. Naujoks, N. D. Spencer, Spatial tuning of the metal work function by means of alkanethiol and fluorinated alkanethiol gradients. *J. Phys. Chem. C* **113**, 5620–5628 (2009).
23. S. van Reenen, S. Kouijzer, R. A. J. Janssen, M. M. Wienk, M. Kemerink, Origin of work function modification by ionic and amine-based interface layers. *Adv. Mater. Interfaces* **1**, 1400189 (2014).
24. T. M. Willey, A. L. Vance, T. van Buuren, C. Bostedt, L. J. Terminello, C. S. Fadley, Rapid degradation of alkanethiol-based self-assembled monolayers on gold in ambient laboratory conditions. *Surf. Sci.* **576**, 188–196 (2005).
25. G. Mani, D. M. Johnson, D. Marton, V. L. Dougherty, M. D. Feldman, D. Patel, A. A. Ayon, C. M. Agrawal, Stability of self-assembled monolayers on titanium and gold. *Langmuir* **24**, 6774–6784 (2008).
26. L. Srisombat, A. C. Jamison, T. R. Lee, Stability: A key issue for self-assembled monolayers on gold as thin-film coatings and nanoparticle protectants. *Colloids Surf. A Physicochem. Eng. Asp.* **390**, 1–19 (2011).
27. P. Tantitarntong, P. Zalar, N. Matsuhisa, K. Nakano, S. Lee, T. Yokota, K. Tajima, T. Someya, High sensitivity tuning of work function of self-assembled monolayers modified electrodes using vacuum ultraviolet treatment. *ACS Appl. Mater. Interfaces* **9**, 28151–28156 (2017).
28. S. Osella, D. Cornil, J. Cornil, Work function modification of the (111) gold surface covered by long alkanethiol-based self-assembled monolayers. *Phys. Chem. Chem. Phys.* **16**, 2866–2873 (2014).
29. N. Crivillers, S. Osella, C. Van Dyck, G. M. Lazzerini, D. Cornil, A. Liscio, F. Di Stasio, S. Mian, O. Fenwick, F. Reinders, M. Neuburger, E. Treossi, M. Mayor, V. Palermo, F. Cacialli, J. Cornil, P. Samorì, Large work function shift of gold induced by a novel perfluorinated azobenzene-based self-assembled monolayer. *Adv. Mater.* **25**, 432–436 (2013).
30. G. Ramanath, M. Kwan, P. K. Chow, Y. C. Quintero, P. H. Mutin, R. Ramprasad, Tuning of noble metal work function with organophosphonate nanolayers. *Appl. Phys. Lett.* **105**, 081601 (2014).
31. S. Lu, Z. Qin, Q. Guo, G. Cao, Work function mediated by deposition of ultrathin polar FeO on Pt (111). *Appl. Surf. Sci.* **392**, 849–853 (2017).
32. J. K. Efavi, T. Mollenhauer, T. Wahlbrink, H. D. B. Gottlob, M. C. Lemme, H. Kurz, Tungsten work function engineering for dual metal gate nano-CMOS. *J. Mater. Sci. Mater. Electron.* **16**, 433–436 (2005).
33. J. Polański, Z. Sidorski, Adsorption of copper on tungsten; measurements on single crystal planes. *Surf. Sci.* **40**, 282–294 (1973).
34. M. E. Grubbs, M. Deal, Y. Nishi, B. M. Clemens, The effect of oxygen on the work function of tungsten gate electrodes in MOS devices. *IEEE Electron Device Lett.* **30**, 925–927 (2009).
35. G. Vida, V. K. Josepovits, M. Győr, P. Deak, Characterization of tungsten surfaces by simultaneous work function and secondary electron emission measurements. *Microsc. Microanal.* **9**, 337–342 (2003).

Acknowledgments

Funding: S.C.T. acknowledges the financial support from the Ministry of Education Academic Research Fund Tier 1 (R-284-000-161-114 and R-284-000-134-112). **Author contributions:** S.K.R. and S.C.T. conceived the concept presented. S.K.R. observed the in-plane photocurrent effect. S.K.R. and S.C.T. designed the experiments. S.K.R. performed the photocurrent and electrical experiments. W.S. provided guidance on the KPFM experiment. S.K.R., W.S., and D.K.N. performed the KPFM experiments. S.K.R. and S.C.T. analyzed and interpreted the data. Y.Z. performed infrared thermography. D.K.N. and Y.Z. also contributed to the discussion of the study. S.K.R and S.C.T. wrote the manuscript. S.C.T. supervised the project. **Competing interests:** The authors declare that they have no competing interests. **Data and materials availability:** All data needed to evaluate the conclusions in the paper are present in the paper and/or the Supplementary Materials. Additional data related to this paper may be requested from the authors.

Submitted 8 August 2017
Accepted 29 January 2018
Published 2 March 2018
10.1126/sciadv.aao6050

Citation: S. K. Ravi, W. Sun, D. K. Nandakumar, Y. Zhang, S. C. Tan, Optical manipulation of work function contrasts on metal thin films. *Sci. Adv.* **4**, eaao6050 (2018).

Science Advances

Optical manipulation of work function contrasts on metal thin films

Sai Kishore Ravi, Wanxin Sun, Dilip Krishna Nandakumar, Yaoxin Zhang and Swee Ching Tan

Sci Adv **4** (3), eaao6050.
DOI: 10.1126/sciadv.aao6050